How To Break the Janus Effect of H_2O_2 in Biocatalysis? Understanding Inactivation Mechanisms To Generate more Robust Enzymes

Zhao, Ze Xin; Lan, Dongming; Tan, Xiyu; Hollmann, Frank; Bornscheuer, Uwe T.; Yang, Bo; Wang, Yonghua

DOI
10.1021/acscatal.8b04948

Publication date
2019

Document Version
Final published version

Published in
ACS Catalysis

ACS Catalysis

Letter

Cite This: ACS Catal. 2019, 9, 2916–2921

pubs.acs.org/acscatalysis

How To Break the Janus Effect of H_2O_2 in Biocatalysis? Understanding Inactivation Mechanisms To Generate more Robust Enzymes

ZeXin Zhao,[†] Dongming Lan,[‡] Xiyu Tan,[‡] Frank Hollmann,[§] Uwe T. Bornscheuer,[∥] Bo Yang,[†] and Yonghua Wang*[,‡]

[†]School of Bioscience and Bioengineering, South China University of Technology, Guangzhou 510006, PR China

[‡]School of Food Sciences and Engineering, South China University of Technology, Guangzhou 510640, PR China

[§]Department of Biotechnology, Delft University of Technology, Van der Maasweg 9, 2629HZ Delft, The Netherlands

[∥]Institute of Biochemistry, Department of Biotechnology and Enzyme Catalysis, Greifswald University, Felix-Hausdorff-Str. 4, 17487 Greifswald, Germany

Supporting Information

ABSTRACT: H_2O_2, is an attractive oxidant for synthetic chemistry, especially if activated as percarboxylic acid. H_2O_2, however, is also a potent inactivator of enzymes. Protein engineering efforts to improve enzyme resistance against H_2O_2 in the past have mostly focused on tedious probabilistic directed evolution approaches. Here we demonstrate that a rational approach combining multiscale MD simulations and Born−Oppenheimer ab initio QM/MM MD simulations is an efficient approach to rapidly identify improved enzyme variants. Thus, the lipase from *Penicillium camembertii* was redesigned with a single mutation (I260R), leading to drastic improvements in H_2O_2 resistance while maintaining the catalytic activity. Also the extension of this methodology to other enzymes is demonstrated.

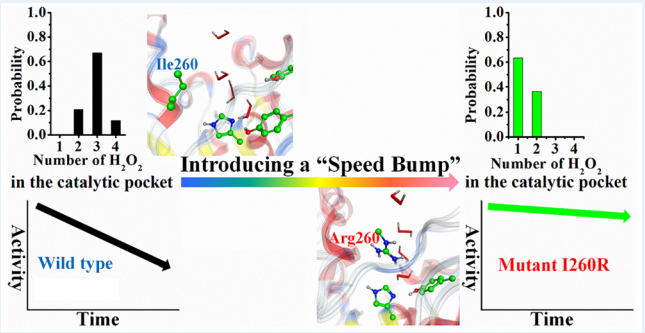

KEYWORDS: *H_2O_2, inactivation, multiscale MD, QM/MM MD, lipase, epoxidation*

The importance of H_2O_2 as oxidant in enzymatic reactions is steadily increasing. For example, peroxygenase-catalyzed reactions and oxidative depolymerization mediated by cofactor free lytic polysaccharide monooxygenases have been gaining increasing attention in the past few years.[1−4] Particularly, the so-called perhydrolase activity of lipases is of significant preparative interest. First, lipases are generally very robust catalysts operating also at elevated temperatures and under nonaqueous conditions. Second, the perhydrolase approach gives access to industrially relevant transformations such as the Baeyer−Villiger oxidation and epoxidation of C=C double bonds (Scheme 1).[5−12]

Furthermore, H_2O_2 is an attractive oxidant, being relatively easy to handle and leaving water as the sole waste product. This makes the chemoenzymatic approach particularly interesting from a preparative point-of-view: instead of using stoichiometric amounts of peracids such as *m*-CPBA, only H_2O_2 and catalytic amounts of the lipase and the carboxylic acid are needed. Overall, this not only results in significant economic savings but also reduces the amount of waste produced significantly.

Nevertheless, despite these attractive features, H_2O_2 also exhibits a "dark side"; the majority of biocatalysts is oxidatively inactivated by H_2O_2, thereby limiting the robustness of H_2O_2-

Scheme 1. Exploiting the Perhydrolase Activity of Lipases To Generate Peracids, Which in Catalytic Amounts Can Perform Baeyer−Villiger Oxidations or Epoxidation (Prilezhaev) Reactions

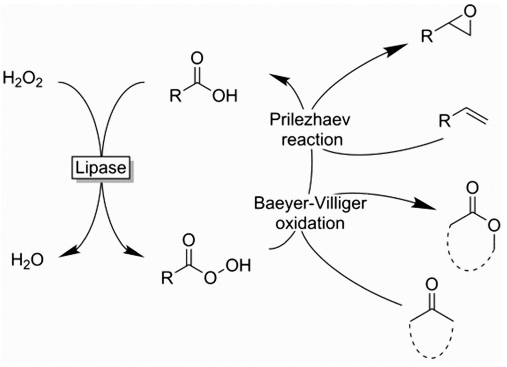

Received: December 11, 2018
Revised: February 19, 2019
Published: February 28, 2019

DOI: 10.1021/acscatal.8b04948
ACS Catal. 2019, 9, 2916−2921

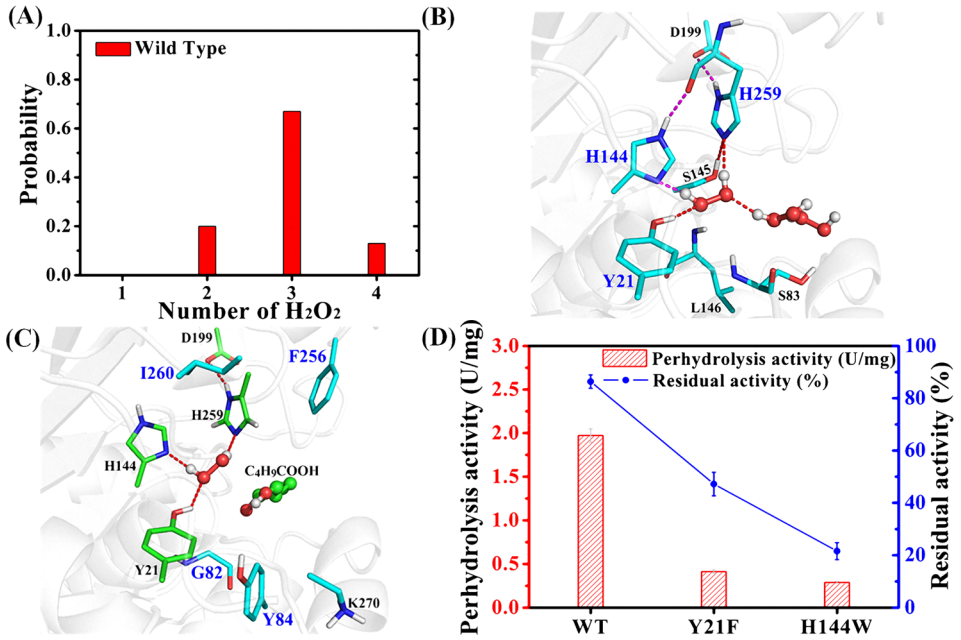

Figure 1. (A) Probabilities of number of H_2O_2 molecules in the catalytic pocket of wild-type model. (B) The geometry conformation of H_2O_2 molecule in the catalytic pocket. (C) The component residues of H_2O_2 binding site (green sticks) and pocket (blue sticks) of PCL. (D) The initial perhydrolysis activity as well as H_2O_2 resistance of wild-type PCL and Y21F, H144W mutants.

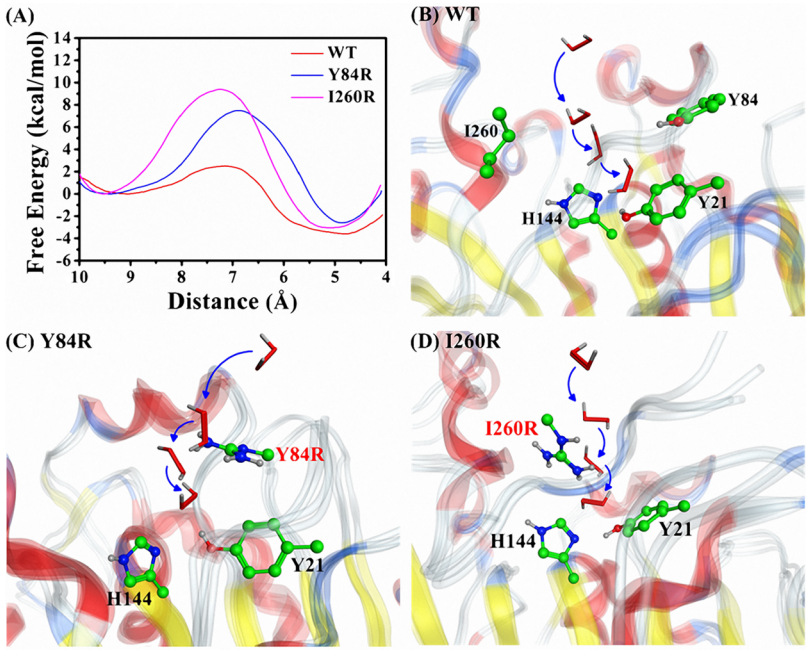

Figure 2. Results of the SMD simulations and umbrella sampling. (A) The distance−energy curves between the mass center of H_2O_2 molecule and Y21/H144 residues in different three models and motion trail of the H_2O_2 molecule from the outside of pocket to the Y21/H144 residues in the (B) wild-type, (C) Y84R, and (D) I260R models, respectively.

driven biocatalytic redox reactions.[13−16] Furthermore, H_2O_2 is also an (undesired) sideproduct of cellular metabolism and may cause adverse side effect. Hence, because of its dual faces, one could compare H_2O_2 with the ancient Roman god of doors and gates, Janus, who was generally depicted with multiple faces.

From an industrial biotechnology point-of-view, improving the H_2O_2 resistance of enzymes is inevitable to attain practical feasibility on an industrial scale.

Immobilization and solvent engineering appear to be promising approaches to alleviate above problem.[8,17−20] However, more elegant would be to engineer enzyme mutants with an increased stability against H_2O_2. Low-redox potential amino acids such as methionine, cysteine, tryptophan, and histidine are plausible targets for protein engineering.[15,21] This has been explored extensively in case of H_2O_2-dependent peroxidases.[22−26] Most mutagenesis studies, however, are based on random strategies such as directed evolution resulting in huge mutant libraries, which are tedious to screen. A rational

DOI: 10.1021/acscatal.8b04948
ACS Catal. 2019, 9, 2916−2921

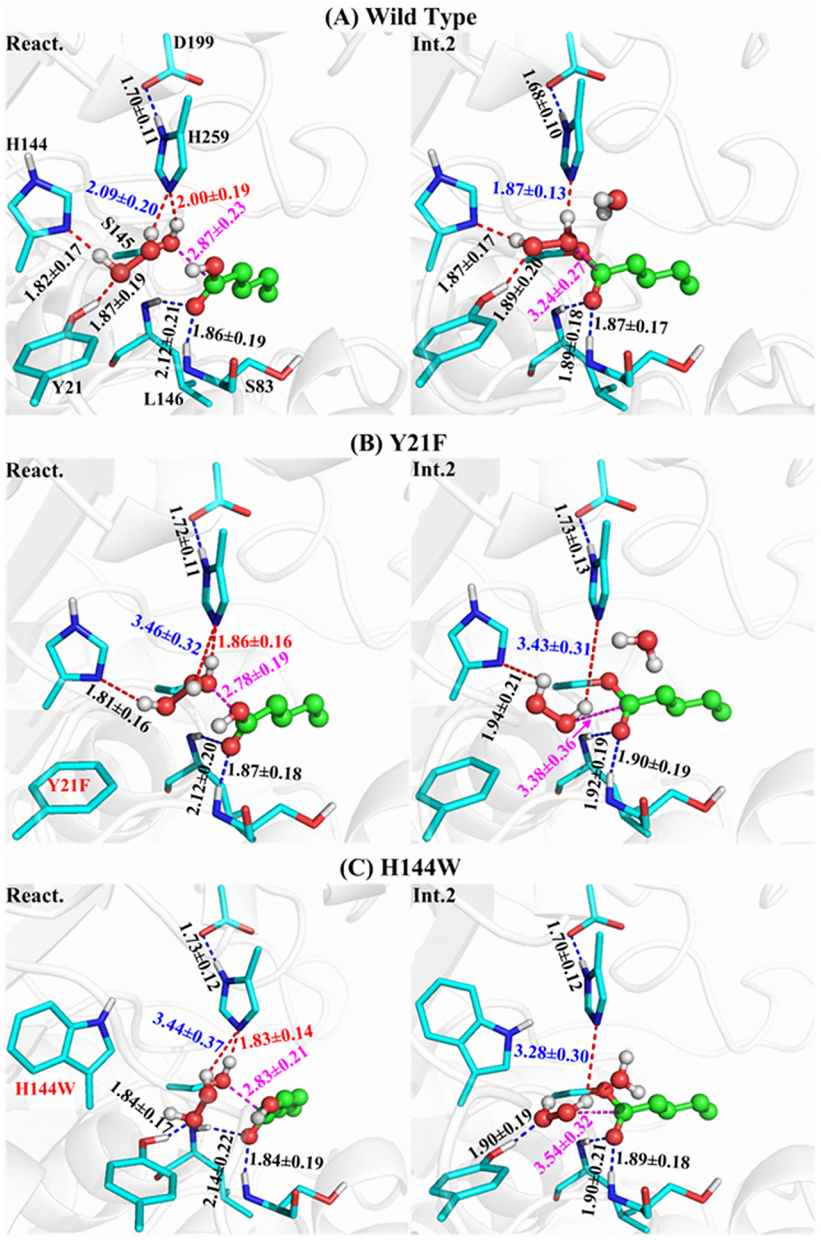

Figure 3. Determined geometries at reactant (React.) and intermediate 2 (Int. 2) of (A) wild-type, (B) Y21F, and (C) H144W models. The unit of the distance data in the figure was Å. The complete reaction processes of the three models were presented in Figure S7−S9.

approach to improve the robustness of enzymes against H_2O_2 has not yet been pursued.

Gaining molecular understanding of the H_2O_2-inactivation mechanism of enzymes may put the basis for a rational approach to design H_2O_2-resistant biocatalysts. To develop such rational strategies, we used the lipase from *Penicillium camembertii* (PCL) as a model enzyme. As a basis for our simulations, we took the crystal structure of PCL.[27]

To elucidate the H_2O_2-inactivation mechanism on PCL, classical molecular dynamic (CMD), steered molecular dynamic (SMD) and Born−Oppenheimer ab initio QM/MM MD were employed (for a detailed description of the methods and the results, please refer to the Supporting Information).[28−35] First, the wild-type PCL model without substrate bound was solvated into a box containing 5000 water molecules and 1000 H_2O_2 molecules followed by a 100 ns CMD simulation. As shown in Figure 1A, in the catalytic pocket can accommodate more than two H_2O_2 molecules, even up to four. It is reasonable to assume that the rate of H_2O_2-related PCL-inactivation correlates with the amount and probability of H_2O_2 found in the enzyme active site.

Further analysis using the CMD trajectory of PCL revealed that the H_2O_2 molecules are preferentially located close to the residues Y21 and H144 (Figure 1B) forming H-bonds with Y21, H144 and H259 (a part of the catalytic triad). The conformation is similar to the binding mode determining by QM/MM MD simulations (Figure 1C; for the detailed process, see section 4 in Supporting Information). To shed light on this, SMD simulations and umbrella sampling were performed to elucidate the H_2O_2 trajectory and the variations of the energy level of H_2O_2 from outside the pocket to the position close to Y21/H144 (Figure 2A,B). This analysis revealed that the binding of H_2O_2 to Y21/H144 is both

DOI: 10.1021/acscatal.8b04948
ACS Catal. 2019, 9, 2916−2921

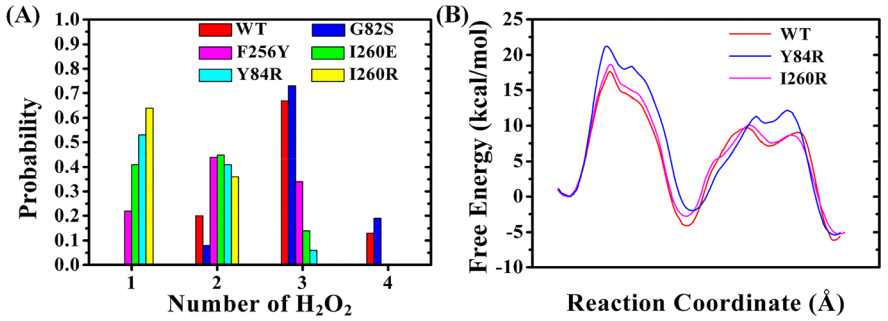

Figure 4. (A) Number of H_2O_2 molecules in the binding pocket of wild-type and various mutant-type models. (B) Complete free-energy profile of the conversion of the pentanoic acid into the corresponding perpentanoic acid for wild-type and mutant-type PCL determined by ab initio QM/MM MD simulations and umbrella sampling (the free-energy profiles see Figure S13).

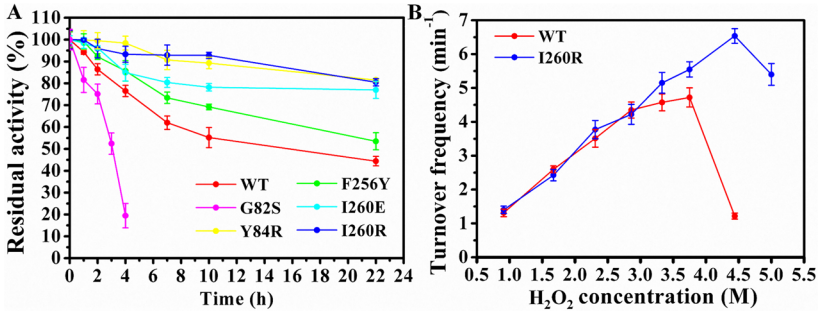

Figure 5. (A) H_2O_2-resistance for the wild-type PCL and various mutant-type PCL. (B) The comparison of the turnover frequency within 12 h between the wild-type PCL and mutant I260R in different H_2O_2 concentration. The detailed comparison of the reaction course referred to Figure S19.

thermodynamically and kinetically favorable. In other words H_2O_2 is "squinted" toward the Y21/H144 residues.

We then carried out an ab initio QM/MM MD simulation with umbrella sampling to further elucidate the catalytic mechanism of PCL and its mutants in the perhydrolysis reaction. The geometries of reactants (i.e., H_2O_2 and pentanoic acid bound to the active site, React.) and intermediate 2 (i.e., H_2O_2 activated by partial deprotonation by H259 attacking the serine-acyl intermediate, Int. 2) are shown in Figure 3A. Again, a strong H-bond network between Y21, H144, and H259 with H_2O_2 was observed controlling its orientation to nucleophilically attack the acyl-enzyme ester (Figure 3A). In React. and Int. 2, the hydrogen bond lengths between H259 and H_2O_2 were 2.09 ± 0.20 Å and 1.87 ± 0.13 Å, respectively. Upon exchanging Y21 or H144 to other amino acids, H_2O_2 becomes more flexible because of significantly increased H-bonding distances and less likely forms a H-bond with H259, which is required for the perhydrolysis of the enzyme-acyl intermediate (Figure 3B,C). The higher degree of freedom of H_2O_2 in such mutants leads to a less efficient perhydrolysis reaction as well as to more interactions of H_2O_2 with other active site residues. As a result, decreased perhydrolysis activity and increaseed susceptibility toward H_2O_2-related inactivation should be the case. This was experimentally conformed (Figure 1D). The perhydrolase activities of e.g. Y21F and H144W (0.41 and 0.29 U/mg for Y21F and H144W, respectively) were significantly lower than the specific activity of the wild-type PCL (1.97 U/mg). Also, both mutants were significantly less stable in the presence of H_2O_2 as compared to the wt-enzyme (loss of 50 or 80% of the initial activity after 2h incubation, respectively, as compared with only 15% loss by the wt-PCL).

On the basis of the above-described H_2O_2-inactivation mechanism, we hypothesized that a promising strategy to increase PCL's resistance against H_2O_2 may be to restrict access of H_2O_2 to the enzyme active site and thereby reducing the amount of H_2O_2 molecules.

To validate this hypothesis, we mutated three nonpolar amino acid residues in the vicinity of the H_2O_2 binding site (G82, F256, and I260) to more polar ones. In addition, we also evaluated the mutant Y84R as the original phenolic OH-group did not appear to contribute to H_2O_2 stabilization as it was pointing away from H_2O_2 and substitution to an arginine may induce more flexibility. Overall, we aimed at mutants with whom H_2O_2 binding is still thermodynamically feasible but kinetically impeded thereby reducing the number of H_2O_2 molecules in the active site. Still these mutants should efficiently bind and position H_2O_2 correctly to act as a nucleophile for the perhydrolysis of the enzyme-acyl compound.

All five mutants were placed in the same water box containing 5000 H_2O and 1000 H_2O_2 molecules followed by 100 ns CMD simulations. Compared to wild-type, mutant G82S did not significantly affect the number of H_2O_2 molecules within the active site (Figure 4A) and the structural stabilization (Figure S11A) thereby not representing an improvement. However, in the case of F256Y, I260E, Y84R, and I260R (Figure 4A) significantly less H_2O_2, in some cases even only one molecule, was observed in the mutants' active sites.

Further CMD analysis of the H_2O_2 trajectory within these mutants revealed that the more polar amino acid residues indeed formed H-bonds with H_2O_2 and thereby kinetically impeded H_2O_2 access to the active site (Figure S11B–E).

DOI: 10.1021/acscatal.8b04948
ACS Catal. 2019, 9, 2916–2921

Again SMD analysis and umbrella sampling were used to investigate the trajectory and energy variation of the H_2O_2 molecule from the outside of the pocket to the mutants. Because of the higher flexibility in C-terminus compared to that of wt-PCL, mutants F256Y and I260E models were no longer considered (Figure S12). As shown in Figure 2A, Y84R and I260R imposed a very significantly higher energy barrier for H_2O_2 to access the active sites as compared to the wt-PCL. This could be assigned to some binding interaction of H_2O_2 with the new, polar amino acid residues (Figure 2C,D), while in case of the wt-PCL H_2O_2, there were no additional impediments. Hence, Y84R and I260R should be more resistant to H_2O_2.

The perhydrolysis mechanism was further elucidated by QM/MM MD simulations. As shown in Figure 4B, a higher activation energy was calculated for the Y84R mutant, while the energy profile for I260R was very comparable to that of the wild-type enzyme. Therefore, we focused on I260R as with this mutant, no significant reduction of the catalytic efficiency was to be expected.

Next, we aimed at experimental validation of the predicted higher robustness especially of I260R. Therefore, we compared the residual activities of wt-PCL and I260R-PCL and some other mutants after incubation in the presence of 1 M H_2O_2 (Figure 5A). Strikingly, while the wt-enzyme lost half of its catalytic activity within 10h, I260R-PCL maintained 80% of its initial activity even after 22h of incubation. Further kinetic characterization of the mutants such as catalytic properties (Table S2), T-, pH-range, thermostability, and acyl donor preference (Figures S16A−D) can be found in the Supporting Information. Here it is worth mentioning that the kinetic parameters for pentanoic acid as acyl donor were almost not affected by the mutations (Table S2). The same is true for the K_M value of H_2O_2. The reaction energy profiles calculated by theoretical prediction of wt-PCL and I260R are similar (Table S3), which is consistent with the experimental results. In the Y84R model, however, the energy barrier for forming the first tetrahedral intermediate (TS. 1) is 3.7 kcal/mol higher than that of wt-PCL (Table S3), which is misaligned with the experimental result. It may be caused by the incorrect side chain orientation introduced in the construction of the model with an open lid (detail analysis see section 6 in Supporting Information). Quite interestingly, I260R not only exhibited a markedly higher resistance toward H_2O_2 as compared with the wt-enzyme, it also had a 16-fold increase half-life time upon incubation at 45 °C (Table S2 and Figure S16C). Possibly, this is due to the formation of a new salt bridge between the newly introduced R260 and D267 (Figure S11E and S15), leading to a stabilization of the C-terminus.

To test the general applicability of our hypothesis we also generated mutants of the lipases from *Aspergillus oryzae* (AOL, PDB: 5XK2) and from *Thermomyces lanuginosus* (TLL, PDB: 1DT3). Particularly the mutants V259R-AOL and L259R-TLL corresponded to the successful I260R mutation in PCL (Figure S17). Again, a substantial improvement in H_2O_2 stability of these mutants compared to their wt-parents was observed while leaving the perhydrolysis activity almost unaltered perhydrolysis activity (Figure S18). These results are also in accordance with a previous report on the stabilization of the esterase from *Pyrobaculum calidifontis*.[36]

Finally, we also compared the catalytic performance of wt- and I260R-PCL in the chemoenzymatic epoxidation of 1-octadecene (Figure 5B and Figure S19). Owing to the high K_M value of both mutants for H_2O_2, a linear rate dependence of both enzymes on the H_2O_2 concentration employed was observed. The wt-enzyme, however, showed a markedly decrease activity (within the time frame of the experiments of 6 h) above 2.8 M H_2O_2, at 4.44 M H_2O_2, the catalytic activity was almost completely lost. I260R, in contrast, exhibited a linearly increasing activity up to 4.44 M H_2O_2. Hence, these results further confirm our hypothesis.

In conclusion, on the basis of extensive multiscale MD simulations and Born−Oppenheimer ab initio QM/MM MD simulations, we have proposed a mechanism for H_2O_2-inactivation of PCL. The mutant I260R proposed from this suggestion also experimentally proved to be more resistant without compromising the catalytic activity. These results could also be transferred to other lipases.

Hence, the approach taken here may be useful one not only for H_2O_2-inactivation of lipases but also for other H_2O_2-dependent biocatalysts as well.

■ ASSOCIATED CONTENT

Supporting Information

The Supporting Information is available free of charge on the ACS Publications website at DOI: 10.1021/acscatal.8b04948.

Computational methods; experimental methods; determination of binding mode; catalytic reaction mechanism; the reactivity difference for Y84R and I260R models; biochemical results for other mutants; Figures S1−S19 and Tables S1−S3; and references (PDF)

■ AUTHOR INFORMATION

Corresponding Author

*E-mail: yonghw@scut.edu.cn.

ORCID

Frank Hollmann: 0000-0003-4821-756X

Uwe T. Bornscheuer: 0000-0003-0685-2696

Yonghua Wang: 0000-0002-3255-752X

Notes

The authors declare no competing financial interest.

■ ACKNOWLEDGMENTS

This work was supported by the National Science Fund for Distinguished Young Scholars (31725022), National Natural Science Foundation of China (31871737), International Collaboration Base for Molecular Enzymology and Enzyme Engineering (2017A050503001), Science and Technology Planning Project of Guangdong Province (2015TX01N207). We thank the National Supercomputing Centers in Shenzhen and Guangzhou for providing the computational resources. We also thank Prof. Yingkai Zhang, Dr. Shenglong Wang at NYU and Prof. Ruibo Wu at SYSU as well as Dr. Jingwei Zhou at GUCM for their help in using QChem-Tinker.

■ REFERENCES

(1) Wang, Y.; Lan, D.; Durrani, R.; Hollmann, F. Peroxygenases en route to becoming dream catalysts. What are the opportunities and challenges? *Curr. Opin. Chem. Biol.* **2017**, *37*, 1−9.

(2) Gomez de Santos, P.; Cañellas, M.; Tieves, F.; Younes, S. H. H.; Molina-Espeja, P.; Hofrichter, M.; Hollmann, F.; Guallar, V.; Alcalde, M. Selective synthesis of the human drug metabolite 5′-hydroxypropranolol by an evolved self-sufficient peroxygenase. *ACS Catal.* **2018**, *8*, 4789−4799.

DOI: 10.1021/acscatal.8b04948
ACS Catal. 2019, 9, 2916−2921

(3) Bissaro, B.; Rohr, A. K.; Muller, G.; Chylenski, P.; Skaugen, M.; Forsberg, Z.; Horn, S. J.; Vaaje-Kolstad, G.; Eijsink, V. G. H. Oxidative cleavage of polysaccharides by monocopper enzymes depends on H_2O_2. *Nat. Chem. Biol.* **2017**, *13*, 1123−1128.
(4) Kuusk, S.; Bissaro, B.; Kuusk, P.; Forsberg, Z.; Eijsink, V. G. H.; Sørlie, M.; Väljamäe, P. Kinetics of H_2O_2-driven degradation of chitin by a bacterial lytic polysaccharide monooxygenase. *J. Biol. Chem.* **2018**, *293*, 523−531.
(5) Wang, X. P.; Zhou, P. F.; Li, Z. G.; Yang, B.; Hollmann, F.; Wang, Y. H. Engineering a lipase B from *Candida antactica* with efficient perhydrolysis performance by eliminating its hydrolase activity. *Sci. Rep.* **2017**, *7*, 44599.
(6) Markiton, M.; Boncel, S.; Janas, D.; Chrobok, A. Highly active nanobiocatalyst from lipase noncovalently immobilized on multi-walled carbon nanotubes for Baeyer−Villiger synthesis of lactones. *ACS Sustainable Chem. Eng.* **2017**, *5*, 1685−1691.
(7) Flourat, A. L.; Peru, A. A. M.; Teixeira, A. R. S.; Brunissen, F.; Allais, F. Chemo-enzymatic synthesis of key intermediates (S)-[γ]-hydroxymethyl-α,β-butenolide and (S)-γ-hydroxymethyl-γ-butyrolactone via lipase-mediated Baeyer-Villiger oxidation of levoglucosenone. *Green Chem.* **2015**, *17*, 404−412.
(8) Ranganathan, S.; Zeitlhofer, S.; Sieber, V. Development of a lipase-mediated epoxidation process for monoterpenes in choline chloride-based deep eutectic solvents. *Green Chem.* **2017**, *19*, 2576−2586.
(9) Aouf, C.; Durand, E.; Lecomte, J.; Figueroa-Espinoza, M.-C.; Dubreucq, E.; Fulcrand, H.; Villeneuve, P. The use of lipases as biocatalysts for the epoxidation of fatty acids and phenolic compounds. *Green Chem.* **2014**, *16*, 1740−1754.
(10) Hua, X.; Xing, Y.; Zhang, X. Enhanced promiscuity of lipase-inorganic nanocrystal composites in the epoxidation of fatty acids in organic media. *ACS Appl. Mater. Interfaces* **2016**, *8*, 16257−16261.
(11) Rauwerdink, A.; Kazlauskas, R. J. How the same core catalytic machinery catalyzes 17 different reactions: the serine-histidine-aspartate catalytic triad of alpha/beta-hydrolase fold enzymes. *ACS Catal.* **2015**, *5*, 6153−6176.
(12) Bernhardt, P.; Hult, K.; Kazlauskas, R. J. Molecular Basis of Perhydrolase Activity in Serine Hydrolases. *Angew. Chem.* **2005**, *117*, 2802−2806.
(13) Albertolle, M. E.; Kim, D.; Nagy, L. D.; Yun, C. H.; Pozzi, A.; Savas, U.; Johnson, E. F.; Guengerich, F. P. Heme-thiolate sulfenylation of human cytochrome P450 4A11 functions as a redox switch for catalytic inhibition. *J. Biol. Chem.* **2017**, *292*, 11230−11242.
(14) Grey, C. E.; Hedström, M.; Adlercreutz, P. A mass spectrometric investigation of native and oxidatively inactivated chloroperoxidase. *ChemBioChem* **2007**, *8*, 1055−1062.
(15) Stadtman, E. R.; Levine, R. L. Free radical-mediated oxidation of free amino acids and amino acid residues in proteins. *Amino Acids* **2003**, *25*, 207−218.
(16) Tornvall, U.; Hedstrom, M.; Schillen, K.; Hatti-Kaul, R. Structural, functional and chemical changes in *Pseudozyma antarctica* lipase B on exposure to hydrogen peroxide. *Biochimie* **2010**, *92*, 1867−1875.
(17) Hernandez, K.; Berenguer-Murcia, A.; Rodrigues, R. C.; Fernandez-Lafuente, R. Hydrogen peroxide in biocatalysis. A dangerous liaison. *Curr. Org. Chem.* **2012**, *16*, 2652−2672.
(18) Moniruzzaman, M.; Kamiya, N.; Goto, M. Biocatalysis in water-in-ionic liquid microemulsions: a case study with horseradish peroxidase. *Langmuir* **2009**, *25*, 977−982.
(19) Stepankova, V.; Bidmanova, S.; Koudelakova, T.; Prokop, Z.; Chaloupkova, R.; Damborsky, J. Strategies for stabilization of enzymes in organic solvents. *ACS Catal.* **2013**, *3*, 2823−2836.
(20) Cui, J.; Cui, L.; Jia, S.; Su, Z.; Zhang, S. Hybrid cross-linked lipase aggregates with magnetic nanoparticles: A robust and recyclable biocatalysis for the epoxidation of oleic acid. *J. Agric. Food Chem.* **2016**, *64*, 7179−7187.
(21) Finnegan, M.; Linley, E.; Denyer, S. P.; Mcdonnell, G.; Simons, C.; Maillard, J. Y. Mode of action of hydrogen peroxide and other oxidizing agents: differences between liquid and gas forms. *J. Antimicrob. Chemother.* **2010**, *65*, 2108−2115.
(22) Ogola, H. J.; Hashimoto, N.; Miyabe, S.; Ashida, H.; Ishikawa, T.; Shibata, H.; Sawa, Y. Enhancement of hydrogen peroxide stability of a novel *Anabaena* sp. DyP-type peroxidase by site-directed mutagenesis of methionine residues. *Appl. Microbiol. Biotechnol.* **2010**, *87*, 1727−1736.
(23) Miyazaki, C.; Takahashi, H. Engineering of the H_2O_2-binding pocket region of a recombinant manganese peroxidase to be resistant to H_2O_2. *FEBS Lett.* **2001**, *509*, 111−114.
(24) Valdivia, A.; Perez, Y.; Dominguez, A.; Caballero, J.; Gomez, L.; Schacht, E. H.; Villalonga, R. Improved anti-inflammatory and pharmacokinetic properties for superoxide dismutase by chemical glycosidation with carboxymethylchitin. *Macromol. Biosci.* **2005**, *5*, 118−123.
(25) Kitajima, S.; Kitamura, M.; Koja, N. Triple mutation of Cys26, Trp35, and Cys126 in stromal ascorbate peroxidase confers H_2O_2 tolerance comparable to that of the cytosolic isoform. *Biochem. Biophys. Res. Commun.* **2008**, *372*, 918−923.
(26) Sáezjiménez, V.; Acebes, S.; Guallar, V.; Martínez, A. T.; Ruizdueñas, F. J. Improving the oxidative stability of a high redox potential fungal peroxidase by rational design. *PLoS One* **2015**, *10*, No. e0124750.
(27) Tang, Q.; Popowicz, G. M.; Wang, X.; Liu, J.; Pavlidis, I. V.; Wang, Y. Lipase-driven epoxidation is a two-stage synergistic process. *Chemistryselect* **2016**, *1*, 836−839.
(28) Case, D. A.; Darden, T. A.; Cheatham, T.E., III; Simmerling, C. L.; Wang, J.; Duke, R. E.; Luo, R.; Walker, R. C.; Zhang, W.; Merz, K. M.; Roberts, B.; Hayik, S.; Roitberg, A.; Seabra, G.; Swails, J.; Götz, A. W.; Kolossváry, I.; Wong, K. F.; Paesani, F.; Vanicek, J.; Wolf, R. M.; Liu, J.; Wu, X.; Brozell, S. R.; Steinbrecher, T.; Gohlke, H.; Cai, Q.; Ye, X.; Wang, J.; Hsieh, M.-J.; Cui, G.; Roe, D. R.; Mathews, D. H.; Seetin, M. G.; Salomon-Ferrer, R.; Sagui, C.; Babin, V.; Luchko, T.; Gusarov, S.; Kovalenko, A.; Kollman, P. A. *AMBER 14*; University of California, San Francisco. 2014.
(29) Adamczyk, A. J.; Cao, J.; Kamerlin, S. C.; Warshel, A. Catalysis by dihydrofolate reductase and other enzymes arises from electrostatic preorganization, not conformational motions. *Proc. Natl. Acad. Sci. U. S. A.* **2011**, *108*, 14115−14120.
(30) Elsässer, B.; Fels, G.; Weare, J. H. QM/MM simulation (B3LYP) of the RNase A cleavage-transesterification reaction supports a triester A_N + D_N associative mechanism with an O2' H internal proton transfer. *J. Am. Chem. Soc.* **2014**, *136*, 927−936.
(31) Kamerlin, S. C.; Mavri, J.; Warshel, A. Examining the case for the effect of barrier compression on tunneling, vibrationally enhanced catalysis, catalytic entropy and related issues. *FEBS Lett.* **2010**, *584*, 2759−2766.
(32) OLsson, M. H.; Siegbahn, P. E. M.; Blomberg, M. R.; Warshel, A. Exploring pathways and barriers for coupled ET/PT in cytochrome coxidase: A general framwork for examing energetics and mechanistic alternatives. *Biochim. Biophys. Acta, Bioenerg.* **2007**, *1767*, 244−260.
(33) Warshel, A. *Computer Modelling of Chemical Reactions in Enzymes and Solutions*; Wiley-Interscience: New York, 1997.
(34) Warshel, A.; Levitt, M. Theoretical studies of enzymic reactions: Dielectric, electrostatic and steric stabilization of the carbonium ion in the reaction of lysozyme. *J. Mol. Biol.* **1976**, *103*, 227−249.
(35) Yue, Y.; Guo, H. Quantum mechanical/molecular mechanical study of catalytic mechanism and role of key residues in methylation reactions catalyzed by dimethylxanthine methyltransferase in caffeine biosynthesis. *J. Chem. Inf. Model.* **2014**, *54*, 593−600.
(36) Zhou, P.; Lan, D.; Popowicz, G. M.; Wang, X.; Yang, B.; Wang, Y. Enhancing H_2O_2 resistance of an esterase from *Pyrobaculum calidifontis* by structure-guided engineering of the substrate binding site. *Appl. Microbiol. Biotechnol.* **2017**, *101*, 5689−5697.

DOI: 10.1021/acscatal.8b04948
ACS Catal. 2019, 9, 2916−2921